Biochemical and Biophysical Research Communications 405 (2011) 19–23

Contents lists available at ScienceDirect

Biochemical and Biophysical Research Communications

journal homepage: www.elsevier.com/locate/ybbrc

Characterization of sarcoplasmic reticulum Ca^{2+} ATPase nucleotide binding domain mutants using NMR spectroscopy

Wazo Myint, Qingguo Gong [1], Jinwoo Ahn, Rieko Ishima *

Department of Structural Biology, University of Pittsburgh School of Medicine, 3501 Fifth Avenue, Pittsburgh, PA 15260, USA

ARTICLE INFO

Article history:
Received 15 December 2010
Available online 25 December 2010

Keywords:
Sarcoplasmic reticulum Ca^{2+} ATPase
Nucleotide binding domain
Structure
NMR

ABSTRACT

Sarcoplasmic reticulum Ca^{2+} ATPase (SERCA) is essential for muscle function by transporting Ca^{2+} from the cytosol into the sarcoplasmic reticulum through ATP hydrolysis. In this report, the effects of substitution mutations on the isolated SERCA-nucleotide binding domain (SERCA-N) were studied using NMR. ^{15}N–^{1}H HSQC spectra of substitution mutants at the nucleotide binding site, T441A, R560V, and C561A, showed chemical shift changes, primarily in residues adjacent to the mutation sites, indicating only local effects. Further, the patterns of chemical shift changes upon AMP–PNP binding to these mutants were similar to that of the wild type SERCA-N (WT). In contrast to these nucleotide binding site mutants, a mutant found in patients with Darier's disease, E412G, showed small but significant chemical shift changes throughout the protein and rapid precipitation. However, the AMP–PNP dissociation constant (~2.5 mM) was similar to that of WT (~3.8 mM). These results indicate that the E412G mutant retains its catalytic activity but most likely reduces its stability. Our findings provide molecular insight into previous clinical, physiological, and biochemical observations.

1. Introduction

The sarco(endo)plasmic Ca^{2+} ATPase (SERCA) is responsible for transporting cytosolic Ca^{2+} into the lumen of the sarcoplasmic reticulum (SR) upon muscle relaxation, through hydrolysis of ATP [1–4]. SERCA dysfunction has been implicated in heart failure [5–7] and in a skin disorder known as Darier's disease [8–12]. Thus, it has been an important target for basic and translational research [7,13,14]. Crystal structures of SERCA at different stages in the Ca^{2+} transport cycle have shown the step-by-step interactions of the three cytosolic domains and the transmembrane domain [15–21]. In the Ca^{2+} pump mechanism, there are two major conformational states, E1 and E2, that allow Ca^{2+} ions to cross from the cytoplasm and luminal sides, respectively [22]. One of the cytosolic domains, SERCA-N, is an ATPase and contains an ATP binding site. This domain plays a major role in the conversion from E1 to E2 and interfaces with the other domains, SERCA-A and SERCA-P.

Previous studies on several mutants of SERCA-N suggest that slight changes of domain conformation can influence both Ca^{2+} transport and ATPase activity, but not necessarily to the same degree. For example, while mutation at the ATP binding site, T441A, reduced both Ca^{2+} transport capacity and ATPase activity to about 50% of the WT level, R560V displayed approximately 60% of the WT Ca^{2+} transport capacity and only 30% of WT ATPase activity [23]. However, mutation at a residue adjacent to R560, C561A, reduced Ca^{2+} transport rate to ca. 80% of WT without affecting ATP binding affinity [23]. Although these apparent discrepancies could be explained by distinct conformational changes in the protein upon mutation of specific residues, an analysis of the conformational impact of these mutations has not been performed. Furthermore, E412G mutation, which has been found in patients with Darier's disease but not in those with heart dysfunction [8–12], has not been analyzed at a structural level. An understanding of the structural consequence of the E412G mutation, which is located in the interior of the N-domain, over 16 Å away from the nucleotide-binding site, may be useful to understand why the mutation does not cause heart dysfunction. Overall, while the structural basis of SERCA phosphorylation and its interactions with phospholamban and the membrane [24–28] have been well characterized, the structural consequences of the N-domain mutations have not been reported.

The isolated SERCA-N domain retains its nucleotide binding activity and its native structure [29–31], and was, therefore, used in the described Circular Dichroism and NMR studies. Specifically, single substitution mutations of E412G, T441A, R560V, or C561A were created to elucidate the effect of each mutation on the SERCA-N structure. Our findings provide atomic level insight into previous biochemical and clinical observations.

* Corresponding author. Address: Room 1037, Biomedical Science Tower 3, 3501 Fifth Avenue, Pittsburgh, PA 15260, USA. Fax: +1 412 648 9008.
E-mail address: ishima@pitt.edu (R. Ishima).
[1] Present address: School of Life Science, University of Science and Technology of China, China.

0006-291X/$ - see front matter © 2010 Elsevier Inc. All rights reserved.
doi:10.1016/j.bbrc.2010.12.094

2. Materials and methods

2.1. Protein expression and purification

The WT SERCA-N sequence (residues 357–660) from rabbit SERCA1a was cloned into a pET15b vector, as described by Mitsu Ikura's group [30], and was modified at the N-terminus to incorporate a tobacco etch virus (TEV) cleavable Poly-Histidine sequence (His_6-tag). The final protein sequence contains an additional three-residue, amino acid sequences of SVD before T357 instead of the GSHM sequence in the previously studied construct [30]. The SERCA-N mutants E412G, T441A, R560V, and C561A were constructed by site directed mutagenesis of the WT plasmid following manufacturer's protocol (Stratagene). The vector was transformed into Rosetta 2 (DE3) cells, and protein was expressed in 1 L cultures of minimal M9 medium with 1 g/L [^{15}N]-NH_4Cl at 18 °C for 16 h by addition of isopropyl β-D-1-thiogalactopyranoside (IPTG) at a final concentration of 0.8–1 mM. For the WT and C561A mutant, additional protein sample was prepared with minimal M9 medium supplemented with 1 g/L [^{15}N]-NH_4Cl and 2 g/L [$^{13}C_6$]-glucose at 37 °C. Proteins in cell lysate in a buffer A (50 mM Sodium Phosphate pH 7.5, 500 mM NaCl, 20 mM Imidazole, 0.02% NaN_3, and 5 mM β-mercaptoethanol) were first purified by applying to a 5 mL HisTrap HP column (GE Healthcare) and then eluting with a buffer containing 500 mM Imidazole in A, The aggregate was removed by a Superdex-75 (GE healthcare) gel filtration chromatography column, equilibrated in buffer B (25 mM Sodium Phosphate pH 7.5, 50 mM NaCl, and 0.02% NaN_3). The His_6-tag was removed by overnight TEV digestion, and proteins were purified by application to a HisTrap HP column (GE Healthcare) at 4 °C. The buffer was exchanged by dialysis to 25 mM Bis–Tris pH 6.5, 150 mM NaCl, 5 mM TCEP, and 0.02% NaN_3 and the proteins were concentrated using Amicon Ultra Centrifugal Filter Units (Millipore) prior to flash freezing by liquid nitrogen. Samples were stored at −80 °C with or without lyophilization.

2.2. Circular Dichroism and UV spectroscopies

Protein samples for Circular Dichroism (CD) spectroscopy measurements were prepared by exchanging the buffer with 20 mM Tris, pH 7.5, and 100 mM NaCl resulting in final protein concentrations of 5–12 μM. The concentrations were determined from three absorbance measurements at 280 nm using the theoretical Beer–Lambert Law extinction coefficient of 13,200 M^{-1} cm^{-1}. Spectra were measured on a J-810 Spectropolarimeter (Jasco Inc., Easton, MD, USA) at 25 °C and averaged over 10 accumulations with a scanning speed of 100 nm/min.

The relative aggregation property at higher protein concentrations was estimated by measuring the amount of protein remaining in the soluble fraction after incubation at 50 °C. Specifically, 30 μl of 100 μM protein in 20 mM Tris, pH 7.5 and 100 mM NaCl were incubated on a 50 °C heat block from 0 to 16 min. Samples were subsequently centrifuged at 4 °C in an Eppendorf FA45-30-11 rotor (Eppendorf, Hauppauge, NY, USA) at 4000 RPM for 20 min. The level of protein in the soluble fraction was determined from absorbance at 280 nm. These experiments were repeated three times to estimate the average and the standard deviation of the residual protein concentrations.

2.3. NMR experiments

All NMR experiments were performed on a Bruker Avance NMR spectrometer equipped with a cryogenic-probe (Bruker Biospin, Billerica, MA, USA) and operating at a ^{1}H Larmor frequency of 600.23 MHz. Protein samples for NMR experiments were prepared in 25 mM Bis–Tris pH 6.5, 150 mM NaCl, 5 mM TCEP, and 0.02% NaN_3 with 5% D_2O at protein concentrations ranging from 242 to 398 μM. ^{15}N–^{1}H heteronuclear single quantum coherence (HSQC) spectra of the WT, E412G, T441A, R560V, and C561A SERCA-N ^{15}N-labeled samples were recorded at 25 °C, unless otherwise noted. The HNCA spectra were recorded for ^{15}N/^{13}C isotope enriched WT and C561A SERCA-N for resonance assignment. For the mutants that exhibited ^{15}N–^{1}H HSQC spectra very similar to that of WT protein, the resonance assignments were estimated by placing the residue assignment from the WT spectrum with the closest peak in the mutant spectrum. ^{15}N–^{1}H HSQC spectra of E412G, T441A, R560V, and C561A SERCA-N were also recorded at different concentrations of AMP–PNP (Adenosine 5′-(β,γ-imido)triphosphate), ranging from 0 to 20 mM, at protein concentrations of 242 μM, 297 μM, 309 μM, 398 μM, and 242 μM, respectively.

All NMR data sets were processed using NMRPipe [32] and analyzed using CARA (www.nmr.ch) [33] and NMRViewJ (One Moon Scientific Inc.) [34]. The weighted net changes in chemical shift between the WT and mutants and those for changes on binding of AMP–PNP were obtained for the ^{15}N and ^{1}H dimensions using the equation: $\Delta\delta = \sqrt{\Delta\delta_H^2 + \left(\frac{\gamma_N}{\gamma_H}\Delta\delta_N\right)}$. Residues that showed $\Delta\delta$ values four times greater than the resolution were considered to have significant $\Delta\delta$. Dissociation constants were estimated from the changes in the $\Delta\delta$ as a function of AMP–PNP concentration.

3. Results

3.1. Effect of mutation on SERCA-N secondary structure

The WT and E412G, T441A, R560V, and C561A proteins could be expressed and purified with reasonable yields, ca. 20 mg/L culture. To confirm that the proteins were folded, CD spectra were recorded for all the mutants as well as for the WT SERCA-N. The spectra in the far-UV region of all the mutants showed an almost identical secondary structural content as the WT (Fig. 1).

To determine whether the substitution mutations altered the thermal stability of the protein, we attempted differential scanning calorimetry. However, due to the precipitation of the samples at high temperature (data not shown), we were unable to obtain useful data. Therefore, thermal stability at high protein concentration (100 μM) was qualitatively evaluated by measuring the amount of soluble protein after incubation at 50 °C (Fig. 1, inset). All SERCA-N

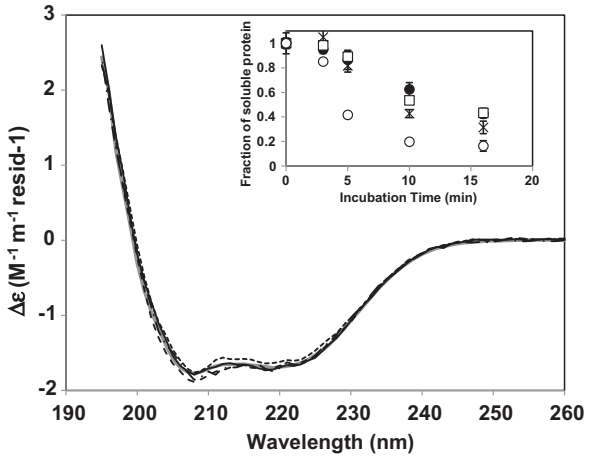

Fig. 1. The Circular Dichroism spectra of the WT (gray solid line), E412G (dashed line), T441A (dotted line), R560V (dot-dashed line), and C561A (black solid line) SERCA-N in 20 mM Tris pH 7.5 and 100 mM NaCl at 25 °C. Inset figure indicates qualitative estimate of protein stability recorded at 50 °C for WT (black circle), T441A (open square), R560 V (cross), and C561A (open circle) SERCA-N mutants (see Section 2).

constructs precipitated sooner than the WT. In particular, the C561A mutant had a greater tendency for precipitation despite the fact that the free cysteine residue was substituted to an alanine. The same experiment was not performed for the E412G mutant, which precipitated even at 25 °C and showed small but significant differences in the signal position in the ^{15}N–^{1}H HSQC spectrum as described later (Fig. 2A).

3.2. Effect of mutation on SERCA-N chemical shifts

The WT SERCA-N ^{15}N–^{1}H HSQC spectrum was almost identical to the spectrum in the previous report by Ikura's group [30]. The only notable differences were in a few residues located at the N-terminal end of the protein, for example T357 and T358, which could be due to the slightly altered sequence employed in our study (see Section 2). Assignments of backbone amide ^{1}H and ^{15}N of the 224 residue resonances were made for the WT protein using an HNCA spectrum and were confirmed by the chemical shift information from the previous study [30].

The ^{15}N–^{1}H HSQC spectra of the WT and mutant proteins exhibited similar patterns of resonance peaks (Figs. 2 and S1), and are consistent with the similarity observed in the CD spectra, indicating that the basic fold of the protein is not altered by the mutations. This observation was also confirmed by ^{15}N transverse relaxation and $\{^{1}H\}$–^{15}N NOE experiments that provided similar profiles for the WT, T441A and C561A proteins (Figure S2). Amide signals in the ^{15}N–^{1}H HSQC spectra of T441A and R560V mutants almost completely overlapped with the WT protein, except for the region around the mutation sites; therefore, most of the backbone amide chemical shifts of the two mutants could be estimated based on the WT assignments (Fig. 2B and C, respectively). The HSQC spectrum of the C561A mutant also showed signals at similar positions to those of WT (Figure S1). However, since some of the C561A signals showed no overlap with the WT (changes in chemical shifts $\Delta\delta \sim 0.3$ ppm), a HNCA experiment was performed to assign signals (Fig. 2D).

E412G mutation caused moderate changes ($\Delta\delta < 0.15$ ppm) in the ^{15}N–^{1}H HSQC signal positions throughout the protein compared to those of WT (Fig. 2A). The protein sample precipitated significantly after a 2 h during HSQC experiment at 25 °C. As described above, the CD spectrum of E412G is almost identical to that of WT. Thus, the observed changes in chemical shifts in the entire protein may be explained by a reduction in the thermal stability of the protein. In other words, the changes in chemical shifts are most likely due to the fast exchange between the major, folded form and the minor, unfolded form. Since the folded WT protein is stable and the mutation site is located within the protein core, the observed precipitation is likely caused by the unfolded form.

3.3. Effect of mutation on AMP–PNP binding

To determine whether the nucleotide binding affinity or binding site is altered by the various mutations, ^{15}N–^{1}H HSQC spectra were recorded at varying concentrations of AMP–PNP, chosen to allow direct comparison of our WT results with those obtained in the previous report [30]. Signal positions in the NMR spectrum of the WT were shifted upon AMP–PNP titration (Fig. 3A), indicating that the exchange is in the fast exchange condition (i.e. the exchange rate is faster than the difference in chemical shifts between the free and bound forms). Significant shifts were observed for residues S423, T441, E442, S488, D490, M494, S495, A517, and L562 (Fig. 3A), all located in the nucleotide-binding pocket. These observations are consistent with those made previously by Ikura's group [30]. However, upon close inspection of the spectra, additional residues were found to be perturbed in response to AMP–PNP binding. These residues included T447 and R476, which are located far from the binding site, approximately 14 Å and 17 Å, respectively, indicating long-range effects of the nucleotide binding (Fig. 4A).

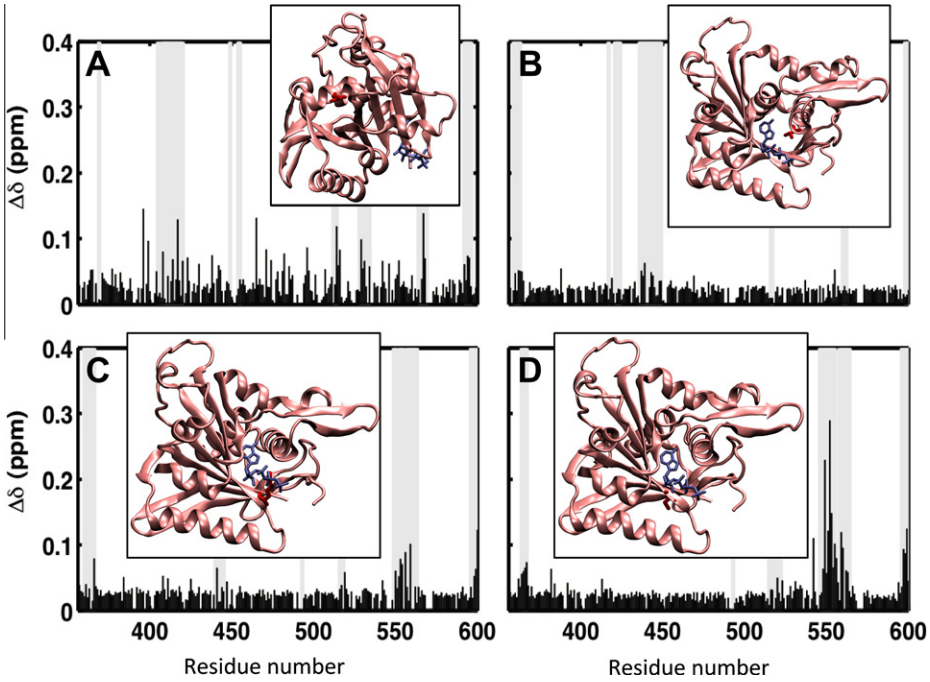

Fig. 2. Differences in amide backbone chemical shifts, $\Delta\delta$, compared to WT SERCA-N for the (A) E412G, (B) T441A, (C) R560V, and (D) C561A mutants are shown with respect to the SERCA1a sequence numbering. The residues within 10 Å of the mutation site are highlighted with gray background bars. Chemical shift changes above 0.0297 ppm are above the resolution of the spectra. In each graph, the mutation site is high-lighted in red and the nucleotide site is shown in purple at the ribbon structure generated (different views were selected for clarification) using PDB code 1IWO (For interpretation of the references to colour in this figure legend, the reader is referred to the web version of this article).

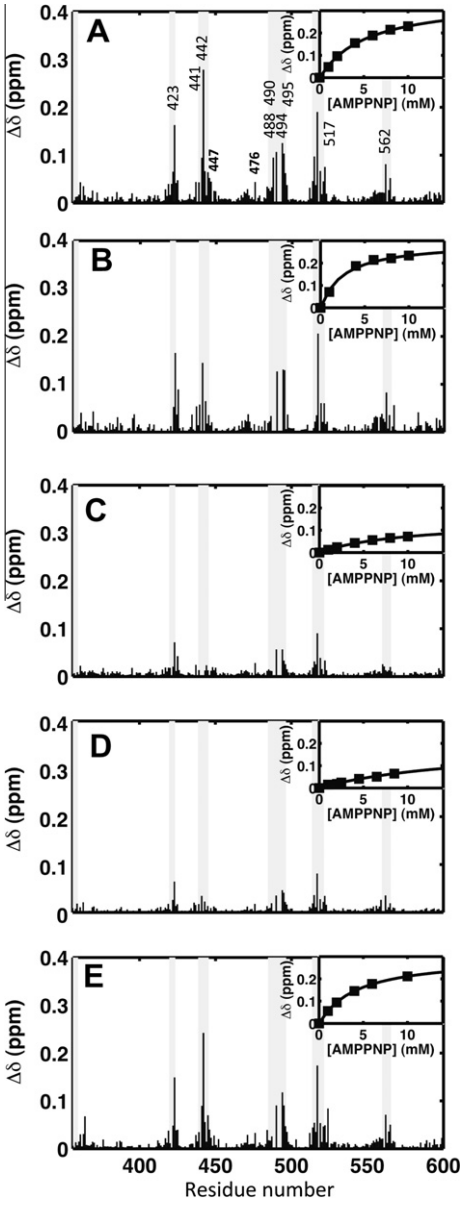

Fig. 3. Differences in amide backbone chemical shifts, $\Delta\delta$, between proteins in the presence of 10 mM AMP–PNP and in the absence of AMP–PNP for the (A) WT, (B) E412G, (C) T441A, (D) R560V, and (E) C561A SERCA-N. The residues within 10 Å of the nucleotide binding site are highlighted with gray background bars. Note that at 10 mM AMP–PNP, the fraction of protein bound to AMP–PNP are 65.8%, 79.9%, 51.3%, <49.5%, and 72.0%, respectively. Insets show the changes in the $\Delta\delta$ as a function of AMP–PNP for residue S423 (black squares).

Using the NMR titration data (Fig. 3, inset), the AMP–PNP dissociation constant, K_D, for the WT protein was estimated to be 5.1 ± 0.8 mM at 25 °C, which is close to the previous estimation by NMR (~2.4 mM, [31]) but larger than the ATP dissociation constant (0.7 mM, [29]). The ATP dissociation constant for the WT protein was determined to be 1.3 ± 0.2 mM (data not shown), very similar to that observed previously.

The AMP–PNP K_D value for the C561A mutant was similar to the WT at 3.80 ± 0.22 mM at 25 °C (Fig. 3E). The K_Ds for the T441A and R560V mutants were smaller than the WT at 9.30 ± 0.54 mM and >10 mM, respectively, at 25 °C (Fig. 3C and D). These tendencies of AMP–PNP dissociation are consistent with the reported reductions in the ATPase activities (100%, 50%, and 30% of WT for

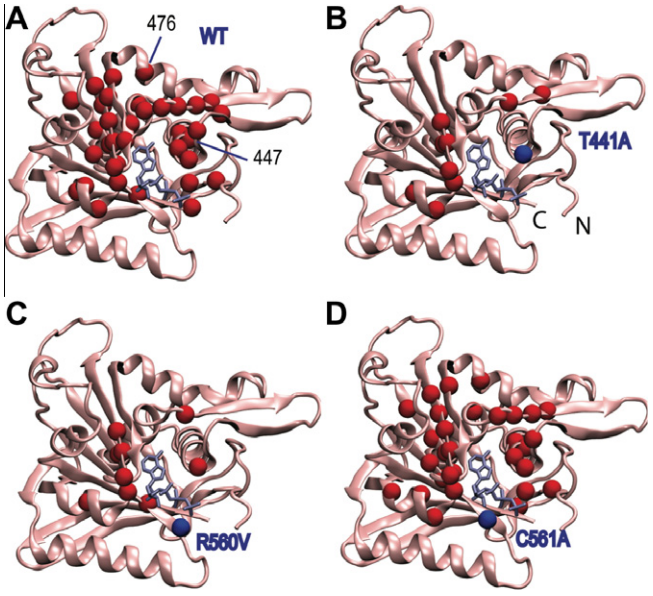

Fig. 4. Illustration of residues (red spheres) with significant chemical shift changes, $\Delta\delta$, upon AMP–PNP binding on a SERCA-N structure (PDB ID: 1IWO) for the (A) WT, (B) T441A, (C) R560V, and (D) C561A mutants. A significant change is considered to be twofold of standard deviations above the average $\Delta\delta$. In B, C, and D, the mutated residues are highlighted as blue spheres. The mapping was not made for the E412G mutant, which exhibited moderate chemical shift changes but was not be assigned due to the instability of the sample. (For interpretation of the references to colour in this figure legend, the reader is referred to the web version of this article.)

C561A, T441A, and R560V, respectively) [23]. The K_D for E412G mutant was estimated to be 2.5 ± 0.2 mM (at 10 °C, to avoid precipitation). Although it cannot be quantitatively compared to that of WT, it is noteworthy that the E412G mutant can bind to AMP–PNP at a qualitatively similar level at low temperature.

4. Discussion

Although mutations that affect the ATPase activity in the SERCA-N domain have been identified [23,35,36], the structural consequences of the mutations have not been reported. The results of this study provide insight into the structure–function relationship of the SERCA ATPase.

The CD spectra (Fig. 1) and the HSQC chemical shift data (Fig. 2) of the T441A, R560V, and C561A SERCA-N mutants indicate that little structural perturbation is present in the mutant proteins. Based on the fact that these mutations did not completely abolish the catalytic activity [23], our observation of such small structural effects is reasonable. Previous crystal structure studies and NMR studies have shown that the SERCA-N domain does not undergo major conformational changes upon nucleotide interaction [15–21]; root mean square deviation (RMSD) of the backbone Cα in the SERCA-N is only 0.6 Å between the E1 and R2 states (calculated using structures of the PDB codes, 3BA6 and 3B9B). Our results confirm that nucleotide binding by these mutants also results primarily in local conformational change, at the binding sites (Figs. 3 and 4). However, small but significant long-range effects were observed upon AMP–PNP binding in both WT and the mutants (Fig. 4), indicating that re-adjustment of the structure occurs in the protein core in the domain study level.

In contrast to these mutants, E412G mutation caused severe protein precipitation at 20 °C. Nevertheless, our data demonstrate that the E412G mutant can bind to AMP–PNP with a similar pattern of chemical shift changes to that of WT at lower temperature suggesting that the E412G mutation may not abolish the nucleo-

tide binding activity. Since the E412G mutation does not cause heart dysfunction [8,10,11], it is reasonable that the E412G mutant still maintains the nucleotide binding activity. However, the E412G mutation is found in the patients with Darier's disease. It has been expected that an alternative mechanism exists to rescue the Ca^{2+}-ATPase function in cardiac muscle [8–12,36,37]. Based on the current results, we propose that such shift of the equilibrium between the native and denatured forms could be rescued by shifting back the equilibrium by other factors.

The C561A mutant exhibited relatively localized changes on chemical shifts compared to the WT protein (Fig. 2D). As described above, such small changes are similar to those of T441A and R560V. However, the C561A mutant has an equivalent AMP–PNP K_D to that of WT (Fig. 3E) and precipitates faster than the T441A, R560V, and WT proteins (Fig. 1, inset). Although significant chemical shift changes throughout the protein were not observed for the C561A mutant, these propensities of C561A mutation are somewhat analogous to those of E412G. Based on this point, the instability of the C561A may relate to the mechanism to maintain the ATPase activity but only causes slight reduction of the Ca^{2+} transport [23].

Acknowledgments

We thank Chang-Hyeock Byeon and Lakshmi Menon for technical help in SERCA-N expression and purification, and Teresa Brosenitsch for critical reading of the manuscript. This study was financially supported by the American Heart Association (Great Rivers affiliate) new investigator grant 0765348U, and National Science Foundation research grant MCB 0814905. Supplementary materials for the HSQC spectra and the relaxation data are available.

Appendix A. Supplementary data

Supplementary data associated with this article can be found, in the online version, at doi:10.1016/j.bbrc.2010.12.094.

References

[1] K.B. Axelsen, M.G. Palmgren, Evolution of substrate specificities in the P-type ATPase superfamily, J. Mol. Evol. 46 (1998) 84–101.
[2] M. Periasamy, S. Huke, SERCA pump level is a critical determinant of Ca^{2+} homeostasis and cardiac contractility, J. Mol. Cell. Cardiol. 33 (2001) 1053–1063.
[3] R. Floyd, S. Wray, Calcium transporters and signalling in smooth muscles, Cell Calcium 42 (2007) 467–476.
[4] M. Brini, E. Carafoli, Calcium pumps in health and disease, Physiol. Rev. 89 (2009) 1341–1378.
[5] U. Schmidt, R.J. Hajjar, P.A. Helm, C.S. Kim, A.A. Doye, J.K. Gwathmey, Contribution of abnormal sarcoplasmic reticulum ATPase activity to systolic and diastolic dysfunction in human heart failure, J. Mol. Cell. Cardiol. 30 (1998) 1929–1937.
[6] C.M. Misquitta, D.P. Mack, A.K. Grover, Sarco/endoplasmic reticulum Ca^{2+}(SERCA)-pumps: link to heart beats and calcium waves, Cell Calcium 25 (1999) 277–290.
[7] P. Muthu, K. Anuradha, SERCA pump isoforms: their role in calcium transport and disease, Muscle Nerve 35 (2007) 430–442.
[8] V.L. Ruiz-Perez, S.A. Carter, E. Healy, et al., ATP2A2 mutations in Darier's disease: variant cutaneous phenotypes are associated with missense mutations, but neuropsychiatric features are independent of mutation class, Hum. Mol. Genet. 8 (1999) 1621–1630.
[9] A. Sakuntabhai, V. Ruiz-Perez, S. Carter, N. Jacobsen, et al., Mutations in ATP2A2, encoding a Ca^{2+} pump, cause Darier disease, Nat. Genet. 21 (1999) 271–277.
[10] F. Ringpfeil, A. Raus, J.J. DiGiovanna, B. Korge, W. Harth, C. Mazzanti, J. Uitto, S.J. Bale, G. Richard, Darier disease – novel mutations in ATP2A2 and genotype–phenotype correlation, Exp. Dermatol. 10 (2001) 19–27.
[11] J. Dhitavat, L. Dode, N. Leslie, A. Sakuntabhai, G. Lorette, A. Hovnanian, Mutations in the sarcoplasmic/endoplasmic reticulum Ca^{2+} ATPase isoform cause Darier's disease, J. Invest. Dermatol. 121 (2003) 486–489.
[12] Y. Miyauchi, T. Daiho, K. Yamasaki, H. Takahashi, A. Ishida-Yamamoto, S. Danko, H. Suzuki, H. Iizuka, Comprehensive analysis of expression and function of 51 sarco(endo)plasmic reticulum Ca^{2+}-ATPase mutants associated with Darier disease, J. Biol. Chem. 281 (2006) 22882–22895.
[13] G. Inesi, A.M. Prasad, R. Pilankatta, The Ca^{2+} ATPase of cardiac sarcoplasmic reticulum: physiological role and relevance to diseases, Biochem. Biophys. Res. Commun. 369 (2008) 182–187.
[14] H.M. Piper, S. Kasseckert, Y. Abdallah, The sarcoplasmic reticulum as the primary target of reperfusion protection, Cardiovasc. Res. 70 (2006) 170–173.
[15] C. Toyoshima, How Ca^{2+}-ATPase pumps ions across the sarcoplasmic reticulum membrane, Biochim. Biophys. Acta 1793 (2009) 941–946.
[16] C. Toyoshima, H. Nomura, Structural changes in the calcium pump accompanying the dissociation of calcium, Nature 418 (2002) 605–611.
[17] C. Olesen, T.L. Sorensen, R.C. Nielsen, J.V. Moller, P. Nissen, Dephosphorylation of the calcium pump coupled to counterion occlusion, Science 306 (2004) 2251–2255.
[18] T.L. Sorensen, J.V. Moller, P. Nissen, Phosphoryl transfer and calcium ion occlusion in the calcium pump, Science 304 (2004) 1672–1675.
[19] C. Olesen, M. Picard, A.-M.L. Winther, C. Gyrup, J.P. Morth, C. Oxvig, J.V. Moller, P. Nissen, The structural basis of calcium transport by the calcium pump, Nature 450 (2007) 1036–1042.
[20] M. Laursen, M. Bublitz, K. Moncoq, C. Olesen, J.V. Moller, H.S. Young, P. Nissen, J.P. Morth, Cyclopiazonic acid is complexed to a divalent metal ion when bound to the sarcoplasmic reticulum Ca^{2+}-ATPase, J. Biol. Chem. 284 (2009) 13513–13518.
[21] A.M. Winther, H. Liu, Y. Sonntag, C. Olesen, M. le Maire, H. Soehoel, C.E. Olsen, S.B. Soehoel, P. Nissen, J.V. Moller, Critical roles of hydrophobicity and orientation of side chains for inactivation of sarcoplasmic reticulum Ca^{2+}-ATPase with thapsigargin and thapsigargin analogs, J. Biol. Chem. 285 (2010) 28883–28892.
[22] M. Makinose, Possible functional states of the enzyme of the sarcoplasmic calcium pump, FEBS Lett. 37 (1973) 140–143.
[23] J.D. Clausen, D.B. McIntosh, B. Vilsen, D.G. Woolley, J.P. Andersen, Importance of conserved N-domain residues Thr441, Glu442, Lys515, Arg560, and Leu562 of sarcoplasmic reticulum Ca^{2+}-ATPase for MgATP binding and subsequent catalytic steps, J. Biol. Chem. 278 (2003) 20245–20258.
[24] D. Guerini, D. Foletti, F. Vellani, E. Carafoli, Mutation of conserved residues in transmembrane domains 4, 6 and 8 causes loss of Ca^{2+} transport by the plasma membrane Ca^{2+} pump, Biochemistry 35 (1996) 3290–3296.
[25] D. Guerini, A. Zecca-Mazza, E. Carafoli, Single amino acid mutations in transmembrane domain 5 confer to the plasma membrane Ca^{2+} pump properties typical of the Ca^{2+} pump of endo(sarco)plasmic reticulum, J. Biol. Chem. 275 (2000) 31361–31368.
[26] G. Nielsen, A. Malmendal, A. Meissner, J.V. Moller, N.C. Nielsen, NMR studies of the fifth transmembrane segment of sarcoplasmic reticulum Ca^{2+}-ATPase reveals a hinge close to the Ca^{2+}-ligating residues, FEBS Lett. 544 (2003) 50–56.
[27] J. Zamoon, F. Nitu, C. Karim, D.D. Thomas, G. Veglia, Mapping the interaction surface of a membrane protein: unveiling the conformational switch of phospholamban in calcium pump regulation, Proc. Natl. Acad. Sci. USA 102 (2005) 4747–4752.
[28] G. Veglia, K.N. Ha, L. Shi, R. Verardi, N.J. Traaseth, What can we learn from a small regulatory membrane protein?, Methods Mol Biol. 654 (2010) 303–319.
[29] P. Champeil, T. Menguy, S. Soulie, B. Juul, A.G. de Gracia, F. Rusconi, P. Falson, L. Denoroy, F. Henao, M. le Maire, J.V. Moller, Characterization of a protease-resistant domain of the cytosolic portion of sarcoplasmic reticulum Ca^{2+}-ATPase, J. Biol. Chem. 273 (1998) 6619–6631.
[30] M. Abu-Abed, T.K. Mal, M. Kainosho, D.H. MacLennan, M. Ikura, Characterization of the ATP-binding domain of the sarco(endo)plasmic reticulum Ca^{2+}-ATPase: probing nucleotide binding by multidimensional NMR, Biochemistry 41 (2002) 1156–1164.
[31] M. Abu-Abed, O. Millet, D.H. MacLennan, M. Ikura, Probing nucleotide-binding effects on backbone dynamics and folding of the nucleotide-binding domain of the sarcoplasmic/endoplasmic-reticulum Ca^{2+}-ATPase, Biochem. J. 379 (2004) 235–242.
[32] F. Delaglio, S. Grzesiek, G.W. Vuister, G. Zhu, J. Pfeifer, A. Bax, NMRPipe: a multidimensional spectral processing system based on UNIX pipes, J. Biomol. NMR 6 (1995) 277–293.
[33] J.E. Masse, R. Keller, AutoLink: automated sequential resonance assignment of biopolymers from NMR data by relative-hypothesis-prioritization-based simulated logic, J. Magn. Reson. 174 (2005) 133–151.
[34] B.A. Johnson, R.A. Blevins, NMR view: a computer program for the visualization and analysis of NMR data, J. Biomol. NMR 4 (1994) 603–614.
[35] N.J. Jacobsen, I. Lyons, B. Hoogendoorn, S. Burge, P.Y. Kwok, M.C. O'Donovan, N. Craddock, M.J. Owen, ATP2A2 mutations in Darier's disease and their relationship to neuropsychiatric phenotypes, Hum. Mol. Genet. 8 (1999) 1631–1636.
[36] B.M. Mayosi, A. Kardos, C.H. Davies, F. Gumedze, A. Hovnanian, S. Burge, H. Watkins, Heterozygous disruption of SERCA2a is not associated with impairment of cardiac performance in humans: implications for SERCA2a as a therapeutic target in heart failure, Heart 92 (2006) 105–109.
[37] S. Tavadia, R.C. Tait, T.A. McDonagh, C.S. Munro, Platelet and cardiac function in Darier's disease, Clin. Exp. Dermatol. 26 (2001) 696–699.